

Efficient Integration of High-Order Stencils into the ADI-FDTD Method

Theodoros T. Zygiridis¹, *Member, IEEE*, Nikolaos V. Kantartzis², *Senior Member, IEEE*,
Christos S. Antonopoulos², *Senior Member, IEEE*, and Theodoros D. Tsiboukis², *Senior Member, IEEE*

¹Dept. of Informatics & Telecommunications Eng., Univ. of Western Macedonia, 50100 Kozani, Greece, tzygiridis@uowm.gr

²Dept. of Electrical and Computer Eng., Aristotle Univ. of Thessaloniki, 54124, Greece, {kant,tsiboukis,chanto}@auth.gr

Incorporating standard high-order spatial approximations in the alternating-direction-implicit (ADI) finite-difference time-domain (FDTD) method does not suffice for accuracy improvement, as these operators are capable of reducing spatial errors only. We herein propose an alternative design procedure, which guarantees finite-difference expressions that minimize the overall space-time flaws. In essence, error formulas are derived from the individual implicit equations, when the ADI update is treated as a single-step process. Then, efficient spatial expressions are extracted via proper manipulations of these formulas that apply error-controlling concepts.

Index Terms—Electromagnetic propagation, error correction, finite-difference methods, numerical stability.

I. INTRODUCTION

UNCONDITIONALLY-STABLE methods [1]–[3] constitute suitable solutions for many problems, as the selection of their temporal resolution depends on accuracy, rather than stability restrictions. Among available schemes, the alternating-direction-implicit (ADI) finite-difference time-domain (FDTD) technique [4] is very popular with attractive features, e.g. it is second-order accurate in time, unlike other approaches (such as the locally-one-dimensional (LOD) scheme [5]). Reliability improvement is always desirable, since this would translate into allowing larger time-steps without any performance penalty.

In this paper, we propose the use of extended spatial stencils to amend the errors of the ADI-FDTD method in two-dimensional (2D) problems. Unlike existing schemes [6], the spatial approximations are now designed to control the overall error, not just the spatial one. To accomplish our goal, different operators are derived for different field components, by exploiting error formulas pertinent to the corresponding update equations. In this manner, significant performance upgrade via simple coefficient modification is accomplished.

II. METHODOLOGY

The application of the classic ADI-FDTD method follows

$$\left(\mathbf{I} - \frac{\Delta t}{2}\mathbf{A}\right) \mathbf{u}|^{n+\frac{1}{2}} = \left(\mathbf{I} + \frac{\Delta t}{2}\mathbf{B}\right) \mathbf{u}|^n \quad (1)$$

$$\left(\mathbf{I} - \frac{\Delta t}{2}\mathbf{B}\right) \mathbf{u}|^{n+1} = \left(\mathbf{I} + \frac{\Delta t}{2}\mathbf{A}\right) \mathbf{u}|^{n+\frac{1}{2}} \quad (2)$$

where $\mathbf{u} = [E_x E_y H_z]^T$ in 2D, \mathbf{I} is the unitary matrix, and \mathbf{A} , \mathbf{B} are 3×3 matrices involving first-order derivatives. We select operators with extended stencils, as a means to introduce design parameters that will enable controlling (and, eventually, improving) the accuracy of the algorithm. Specifically, the finite-difference approximations have the form

$$D_u^w u|_i = \frac{1}{\Delta u} \sum_{\ell=1}^2 C_{u,\ell}^w \left(u|_{i+\ell-\frac{1}{2}} - u|_{i-\ell+\frac{1}{2}} \right) \quad (3)$$

where w denotes correspondence to either electric (e) or magnetic (m) components, and $u \in \{x, y\}$ indicates the axis

of differentiation. Then, \mathbf{A} and \mathbf{B} are written as

$$\mathbf{A} = \begin{bmatrix} 0 & 0 & \frac{1}{\epsilon} D_y^m \\ 0 & 0 & 0 \\ \frac{1}{\mu} D_y^e & 0 & 0 \end{bmatrix}, \mathbf{B} = - \begin{bmatrix} 0 & 0 & 0 \\ 0 & 0 & \frac{1}{\epsilon} D_x^m \\ 0 & \frac{1}{\mu} D_x^e & 0 \end{bmatrix}$$

Since intermediate values $\mathbf{u}|^{n+\frac{1}{2}}$ are not calculated accurately, we treat the algorithm as a single-step approach:

$$\underbrace{\left(\mathbf{I} - \frac{\Delta t}{2}\mathbf{A}\right) \left(\mathbf{I} - \frac{\Delta t}{2}\mathbf{B}\right)}_{\mathbf{M}} \mathbf{u}|^{n+1} = \underbrace{\left(\mathbf{I} + \frac{\Delta t}{2}\mathbf{A}\right) \left(\mathbf{I} + \frac{\Delta t}{2}\mathbf{B}\right)}_{\mathbf{N}} \mathbf{u}|^n \quad (4)$$

where

$$\mathbf{M} = \begin{bmatrix} 1 & -\frac{(c_0\Delta t)^2}{4} D_y^m D_x^e & -\frac{\Delta t}{2\epsilon} D_y^m \\ 0 & 1 & \frac{\Delta t}{2\epsilon} D_x^m \\ -\frac{\Delta t}{2\mu} D_y^e & \frac{\Delta t}{2\mu} D_x^e & 1 \end{bmatrix} \quad (5)$$

$$\mathbf{N} = \begin{bmatrix} 1 & -\frac{(c_0\Delta t)^2}{4} D_y^m D_x^e & \frac{\Delta t}{2\epsilon} D_y^m \\ 0 & 1 & \frac{\Delta t}{2\epsilon} D_x^m \\ \frac{\Delta t}{2\mu} D_y^e & -\frac{\Delta t}{2\mu} D_x^e & 1 \end{bmatrix} \quad (6)$$

As seen, there exist two terms involving the mixed operator $D_y^m D_x^e$, which render the ADI-FDTD method a perturbation of the Crank-Nicolson approach, since only two of the three equations comply to the latter discretization scheme.

Let's first consider the E_y calculation. A description of the pertinent error can be found by admitting plane-wave solutions for the field components. Specifically, if ϕ is the direction of wave propagation and $H_z = H_0 e^{j(\omega t - \mathbf{k}\cdot\mathbf{r})}$, then $E_y = \eta H_0 e^{j(\omega t - \mathbf{k}\cdot\mathbf{r})} \cos \phi$, where \mathbf{k} is the wave-vector, ω the angular frequency, and η the characteristic impedance of the background medium. The update equation is then written as $\Lambda_x^m(\tilde{N}, Q, R, \phi) = 0$, where $\tilde{N} = \tilde{\lambda}/\Delta x$ is the grid density (with respect to the numerical wavelength), Q determines the time-step size via $Q = c_0 \Delta t \sqrt{\Delta x^{-2} + \Delta y^{-2}}$, and $R = \Delta y/\Delta x$. By introducing the exact wavelength instead, we obtain the non-vanishing quantity $\Lambda_x^m(N, Q, R, \phi)$,

$$\Lambda_x^m(N, Q, R, \phi) = \sum_{\ell=1}^2 C_{x,\ell}^m \sin \left[(2\ell - 1) \frac{\pi}{N} \cos \phi \right]$$

$$-\frac{\sqrt{1+R^2}}{QR} \tan\left(\frac{\pi QR}{N\sqrt{1+R^2}}\right) \cos\phi \quad (7)$$

which is characteristic of the entailed numerical error. To calculate the unknown coefficients, we derive the aforementioned formula's trigonometric expansion, by exploiting

$$\sin(\alpha \cos\theta) = 2 \sum_{m=0}^{\infty} (-1)^m J_{2m+1}(\alpha) \cos[(2m+1)\phi] \quad (8)$$

where J_n is the first kind, n -th order Bessel function. Then, the vanishing of the first two terms produces two equations that determine the form of the D_x^m operator:

$$\begin{bmatrix} J_1\left(\frac{\pi}{N}\right) & J_1\left(\frac{3\pi}{N}\right) \\ J_3\left(\frac{\pi}{N}\right) & J_3\left(\frac{3\pi}{N}\right) \end{bmatrix} \begin{bmatrix} C_{x,1}^m \\ C_{x,2}^m \end{bmatrix} = \begin{bmatrix} \frac{\sqrt{1+R^2}}{2QR} \tan\left(\frac{\pi QR}{N\sqrt{1+R^2}}\right) \\ 0 \end{bmatrix}$$

Interestingly, we find that the new coefficients attain the values of the standard fourth-order operators, in the limit case $N \rightarrow +\infty$, as it is $C_1^m = \frac{9}{8} + O\left(\frac{1}{N^2}\right)$ and $C_2^m = -\frac{1}{24} + O\left(\frac{1}{N^2}\right)$.

The same approach is applied to the third update equation, which involves both x - and y -derivatives for electric field components. The definition of another error formula and the elimination of (now four) terms in its trigonometric expansion generates optimized versions of the D_x^e and D_y^e operators.

In the last step, the construction of D_y^m from the first update equation is performed. In this case, a more complicated formula Λ_y^m is derived, owing to the presence of the additional (mixed derivative) terms. Now, the first harmonics ($\Lambda_y^m = \Lambda_{y,1}^m \sin\phi + \Lambda_{y,3}^m \sin(3\phi) + \dots$) are obtained numerically, rather than analytically, by applying the well-known formula

$$\Lambda_{y,\ell}^m = \frac{1}{\pi} \int_0^{2\pi} \Lambda_y^m \sin(\ell\phi) d\phi, \quad \ell = 1, 3, \dots \quad (9)$$

III. PERFORMANCE ASSESSMENT

First, the spectral properties of the modified algorithm are examined by means of the errors affecting the numerical phase velocity. The latter is calculated from the dispersion relation, which is obtained from (4), after setting $\mathbf{u} = \mathbf{u}_0 e^{j(\omega t - \mathbf{k} \cdot \mathbf{r})}$ and requiring the existence of non-trivial solutions:

$$\frac{16 \tan^2\left(\frac{\omega \Delta t}{2}\right)}{(c_0 \Delta t)^2} = (c_0 \Delta t)^2 R_x^e R_x^m R_y^e R_y^m - 4(R_x^e R_x^m + R_y^e R_y^m) \quad (10)$$

where

$$R_u^w = -\frac{2j}{\Delta u} \sum_{\ell=1}^2 C_{u,\ell}^w \sin\left(\frac{2\ell-1}{2} k_u \Delta u\right) \quad (11)$$

If the proposed approach is valid, the error should exhibit low levels, at least at the frequency where the procedure is performed. Table I presents the error in the phase velocity, averaged over $[0, 2\pi)$, for standard and novel ADI-FDTD schemes. We select $Q = 15$, $R = 1$, and grid densities corresponding to $40m$, $m = 1, 2, 4, 8$, cells per wavelength. Similarly to our initial observations, the results verify that the use of fourth-order approximations makes little difference, compared to the second-order approach, especially for high Q values. On the other hand, the error is reduced significantly

TABLE I
OVERALL ERROR FOR VARIOUS METHODS AND MESH RESOLUTIONS

cpw	2nd-order	4th-order	Proposed
40	1.97×10^{-1}	1.96×10^{-1}	6.46×10^{-3}
80	4.77×10^{-2}	4.75×10^{-2}	3.83×10^{-4}
160	1.18×10^{-2}	1.18×10^{-2}	2.40×10^{-5}
320	2.95×10^{-3}	2.94×10^{-3}	1.51×10^{-6}

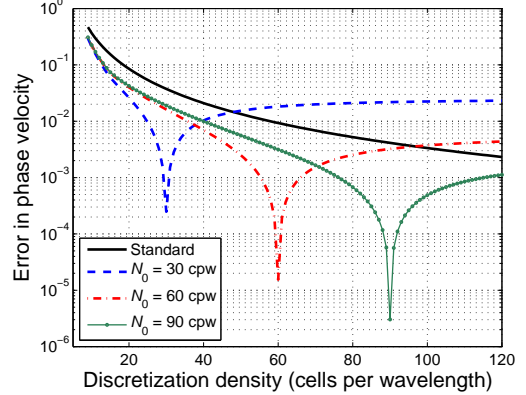


Fig. 1. Overall error in numerical phase velocity versus mesh discretization density (in cells per wavelength – cpw) for various cases.

when the new operators are applied, and converges at a fourth-order rate, despite the second-order accuracy in time.

The effect of the new operators on the wideband performance of the ADI-FDTD method is depicted in Fig. 1, where the error in the phase velocity is plotted over a range of discretizations ($Q = 5$, $R = 1$). The cases where the design frequency corresponds to $N_0 = 30, 60$, or 90 cells per wavelength are shown, against the standard fourth-order expressions. The appearance of sharp minima at the design points validates again the consistency of the proposed approach. In addition, the adoption of the modified expressions does not compromise the algorithm's broadband response, since substantial improvement is also identified over an extended frequency range.

Numerical results from test simulations will be included in the full version of the paper. Preliminary simulations of a rectangular resonant cavity supporting three different modes exhibit error reduction by at least an order of magnitude.

REFERENCES

- [1] R. Qiang, D. Wu, Ji Chen, S. Wang, D. Wilton, and W. Kainz, "An efficient two-dimensional FDTD method for bio-electromagnetic applications," *IEEE Trans. Magn.*, vol. 42, no. 4, pp. 1391-1394, Apr. 2006.
- [2] C. T. M. Choi and S.-H. Sun, "Simulation of axon activation by electrical stimulation—applying alternating-direction-implicit finite-difference time-domain method," *IEEE Trans. Magn.*, vol. 48, no. 2, pp. 639-642, Feb. 2012.
- [3] Md. M. Rana and A. S. Mohan, "Segmented-locally-one-dimensional-FDTD method for EM propagation inside large complex tunnel environments," *IEEE Trans. Magn.*, vol. 48, no. 2, pp. 223-226, Feb. 2012.
- [4] T. Namiki, "A new FDTD algorithm based on alternating direction implicit method," *IEEE Trans. Microw. Theory Tech.*, vol. 47, no. 10, pp. 2003-2007, Oct. 1999.
- [5] J. Shibayama, M. Muraki, J. Yamauchi and H. Nakano, "Efficient implicit FDTD algorithm based on locally one-dimensional scheme," *Electron. Lett.*, vol. 41, no. 19, pp. 1046-1047, Sept. 2005.
- [6] Z. Wang, J. Chen, and Y. Chen, "Development of a higher-order ADI-FDTD method," *Microw. Opt. Technol. Lett.*, vol. 37, no. 1, pp. 8-12, Apr. 2003.